Constructal Theory in Heat Transfer

7

Luiz A. O. Rocha, S. Lorente, and A. Bejan

Contents

1 Introduction 330
2 Fundamentals of Constructal Theory in Heat Transfer 331
2.1 Constructal Law, Constructal Theory, and Vascularization 332
2.2 Thermal Resistance 332
2.3 Imperfection 333
2.4 Constructal Design Method 333
3 Configurations for Open Cavities 334
3.1 Isothermal Elemental Open Cavity 334
3.2 Complex Cavities 339
4 Flow Spacings 350
5 Trees for Heat Conduction 350
6 Constructal Invasion of a Conducting Tree into a Conducting Body 355
7 The Effect of Size on the Design of Distributed Heating on the Landscape 356
8 Conclusions 357
9 Cross-References 358
References 359

L. A. O. Rocha (✉)
Departamento de Engenharia Mecânica, Universidade Federal do Rio Grande do Sul, Porto Alegre, RS, Brazil
e-mail: laorocha@gmail.com

S. Lorente
Departement de Genie Civil, Institut National des Sciences Appliquées, Toulouse, France
e-mail: lorente@insa-toulouse.fr

A. Bejan
Department of Mechanical Engineering and Materials Science, Duke University, Durham, NC, USA
e-mail: abejan@duke.edu

F. A. Kulacki (ed.), *Handbook of Thermal Science and Engineering*,
https://doi.org/10.1007/978-3-319-26695-4_66

Abstract

The Constructal Law is the law of physics that accounts for the universal phenomenon of evolution of flow configuration in nature. Evolution and the Constructal Law unite all the "live" systems, bio and nonbio, which are characterized by flow and freedom to morph. The Constructal Law is the time direction of the evolution phenomenon, namely, toward configurations that offer greater access to the currents of the live system. A constructer theory is the use of the Constructal Law for the purpose of predicting how a particular phenomenon of evolution will unfold. Constructal design is the philosophy of evolutionary design in engineering applications. In this chapter, the law, the theory, and the design are illustrated with examples from the field of heat transfer: vascular flow architectures, tree shaped cavities, conductive inserts for cooling, and networks for distributed heating on the inhabited landscape. In sum, this chapter makes the case for the central role played by theory and design in science.

1 Introduction

A law of physics is a concise statement that summarizes a phenomenon that occurs in nature. The Constructal-Law field started from the realization that "design" is a universal physics phenomenon. It unites the animate with the inanimate over an extremely broad range of scales, from the tree design of the snowflake to animal design and the tree design of the Amazon River basin. The concepts of life, design, and future (evolution) were placed firmly in physics by the Constructal Law, stated in 1996 (Bejan 1996a).

> For a finite-size flow system to persist in time (to live), its configuration must evolve in such a way that provides greater and greater access to the currents that flow through it.

According to the Constructal Law, a live system is one that has two universal characteristics: It flows (i.e., it is a nonequilibrium system in thermodynamics) and it morphs freely toward configurations that allow all its currents to flow more easily over time. Life and evolution are a physics phenomenon, and they belong in physics (Bejan 2016).

To see the position of design in nature as a universal phenomenon of physics, it is necessary to recall that thermodynamics rests mainly on two laws, which are both "first principles." The first law commands the conservation of energy in any system. The second law commands the presence of irreversibility (i.e., the generation of entropy) in any system: By itself, any stream flows naturally one way, from high to low. The permanence and extreme generality of the two laws are consequences of the fact that in thermodynamics the "any system" is a black box. It is a region of space, or a collection of matter without specified shape and structure. The two laws are global statements about the balance or imbalance of the flows (mass, heat, work, entropy) that flow into and out of the black box. Nature is not made of boxes without configuration. The systems that we discern in nature have shape and structure. They

are macroscopic, finite size, and recognizable as patterns – sharp lines on a diffuse background. They have configurations, maps, rhythms, and sounds. They are simple: Their complexity is modest, because if it were not modest we would not be able to discern them and to question their existence. The very fact that they have names (river basins, blood vessels, trees) indicates that they have unmistakable appearances.

Bejan (1996a) drew attention to the fact that the laws of thermodynamics do not account completely for the systems of nature, even though scientists have built thermodynamics into thick books in which the two laws are just the introduction. The body of thermodynamics is devoted to describing, designing, and optimizing things that seem to correspond to systems found in nature, or to devices that can be used by humans to make life easier. Nowhere is this more evident than in engineering, where the method of entropy generation minimization (Bejan 1982, 1996b) is recognized as thermodynamics, even though neither of the two laws accounts for the natural occurrence of "design" or "optimization" phenomena.

If physics is to account for the systems of nature completely, then thermodynamics must be strengthened with an additional self-standing law (i.e., with another first principle) that covers all phenomena of design occurrence and evolution. This addition to physics is the Constructal Law.

The Constructal Law is not a statement of optimization, maximization, minimization, or any other mental image of "end design" or "destiny." The Constructal Law is about the direction of evolution in time and the fact that the design phenomenon is not static: It is dynamic, ever changing, like the images in a movie at the cinema. Evolution never ends. The time direction is the natural phenomenon, and the law of physics that governs this natural phenomenon is the Constructal Law.

Constructal design is the philosophy of evolutionary design in engineering applications. In this chapter, the law, the theory, and the design are illustrated with examples from the field of heat transfer: vascular flow architectures, tree shaped cavities, conductive inserts for cooling, and networks for distributed heating on the inhabited landscape. There is no "best" in evolutionary design. There is "better" today, which turns out to be not as good tomorrow. Constructal design is not a mathematical optimization method. However, when the system has many degrees of freedom, the Constructal design method can be used in association with some optimization methods, for example, exhaustive search or genetic algorithm (Lorenzini et al. 2014a). This approach makes possible to study complex systems, that is, systems with a larger number of degrees of freedom. Constructal design will be used in the examples of this chapter. In sum, this chapter makes the case for the central role played by theory and design in science.

2 Fundamentals of Constructal Theory in Heat Transfer

According to Bejan and Lorente (2008) a flow system has a finite size (it is not infinitesimal) and houses the movement of one entity relative to another (background). It is described by *what* the flow carries (fluid, heat, or mass), *how much* it carries (mass flow rate, heat current, etc.), and *where* the stream is located on its background.

Constructal theory focuses on the *where* because a flow system has *design* (configuration, drawing). The emergence of the flow configuration is understood as a physics phenomenon that is based on a physics principle, the Constructal Law.

2.1 Constructal Law, Constructal Theory, and Vascularization

Constructal theory is the view that flow configuration (geometry, design) can be reasoned on the basis of a principle of configuration generation and evolution in time toward greater global flow access in systems that are free to morph (Bejan 1996b, c). That principle is the Constructal Law.

Constructal Law is a law of physics: "For a finite-size flow system to persist in time (to live), its configuration must change in time such that it provides easier and easier access to its currents (fluid, energy, species, etc.)" (Bejan and Lorente 2008).

Vascularized is a good name for the complex energy systems that new thermal sciences are covering. Vascularized is everything, the animate, the inanimate, and the engineered, from the muscle and the river basin to the cooling of high-density electronics (Bejan and Lorente 2008). A vascular architecture consists of one or more tree-shaped flows, each connecting a point with an area or volume.

2.2 Thermal Resistance

Conduction, or thermal diffusion, occurs when two bodies touch and when there is no bulk motion in either body. The simplest example is a two-dimensional slab of surface A and thickness L. One side of the slab is at temperature T_1 and the other at T_2. The slab is the body across which the two entities (at T_1 and T_2) make thermal contact. The thermal conductivity of the slab material is k. The total heat current across the slab, from T_1 to T_2, is described by the Fourier's law of heat conduction,

$$q = k\frac{A}{L}(T_1 - T_2) \tag{1}$$

The group kA/L is the thermal conductance of the configuration (the slab). The inverse of this group is the thermal resistance of the slab,

$$R_t = \frac{T_1 - T_2}{q} = \frac{L}{kA} \tag{2}$$

There is a huge diversity of body-body thermal contact configurations, and thermal resistances are available in the literature (Bejan 1993).

Convection is said to be external when a much larger space filled with flowing fluid (the free stream) exchanges heat with a body immersed in the fluid. The objective of the analysis is to determine the relation between the heat transfer rate (or the heat flux through a spot on the wall, q'') and the wall-fluid temperature

difference ($T_w - T_\infty$). The alternative is to determine the convective heat transfer coefficient h, which for the external flow is defined by

$$h = \frac{q''}{T_w - T_\infty} \tag{3}$$

where q'' is the heat flux, $q'' = q/\mathrm{A}$, where A is the area swept by the flowing fluid. This means that the heat transfer rate can be written as

$$q = hA(T_w - T_\infty) \tag{4}$$

or that the convective thermal resistance is

$$R_t = \frac{T_w - T_\infty}{q} = \frac{1}{hA} \tag{5}$$

The order of magnitude of h for various classes of convective heat transfer configurations, as well as several numerical or empirical correlations, can be found in Bejan (1993).

2.3 Imperfection

The concept of imperfection for heat transfer is an integral part of thermodynamics and the design method of entropy generation minimization (Bejan 1982, 2000). For example, consider a high thermal conductivity pathway inserted into a finite body of low thermal conductivity which generates heat per unit of volume. The heat flows from the body to the rim, that is, a lower temperature. The two modes of flowing with imperfection (irreversibility), the interstices and the links, must be balanced so that together they ease the global flow. The flow architecture is the graphical expression of the balance between channels (pathways) and their interstices. The deduced architecture (tree, spacing, etc.) is the distribution of imperfection over the available flow space. It is the architecture for access into and out of the flow space, which is finite. Those who model natural trees and then draw them as black lines on white paper (while not struggling to discover the layout of every black line on its allocated white patch) miss half of the drawing. The white is as important as the black. Imperfections can be decreased, but not eliminated. Better configurations are achieved when imperfections are optimally distributed into the system.

2.4 Constructal Design Method

The Constructal Law is applied using the Constructal Design Method, also known as Design with Constructal Theory (DCT) (Bejan and Lorente 2008). The method consists of the following steps (Bejan, interviewed by Kosner 2012):

1. *Define Your System*: Identify clearly and unambiguously what constitutes your "system," that is, the region in space, or the amount of mass that is the subject of your thinking, analysis, and design.
2. *Identify the Flows*: Make sure your system has the freedom to change, and that you understand "what flows" within it, that is, why your system is a "flow system."
3. *Start Simple*: Allow only one feature of your system to change at first. This endows your system with one degree of freedom. Study if and how changes to this feature increase the flow access of the currents that inhabit your system. Incorporate the first feature with which you found that your system performs best into your design (be alert, this is not the end!)
4. *Add a Degree of Freedom*: Allow a second feature to change freely. As you investigate this second degree of freedom, you will find another best feature and adopt it. With this second feature in place, go back to step 3 and refine that first feature to work with the second.
5. *And Another*: Allow a third feature to vary freely, find the best variant of this feature, and then go back and repeat steps 3 and 4, that is, refine the preceding two features.
6. *And So On*: This is a construction process with no end, except the finite time of the investigator.

There is no "best" in evolutionary design. There is "better" today, which turns out to be not as good tomorrow. DCT is not a mathematical optimization method. When the system has many degrees of freedom, the Constructal design method can be used in association with some optimization methods, for example, exhaustive search or genetic algorithm (Lorenzini et al. 2014a). This approach makes possible to study complex systems, that is, systems with a larger number of degrees of freedom. Constructal design will be applied in the examples of this chapter.

3 Configurations for Open Cavities

This section illustrates how to discover the shape of open cavities that intrudes into a solid conducting wall. The cavity can also be seen as "negative fin" or "inverted fin" because its shape would be generated if a fin is inserted into the body and its volume removed from the solid body. Open cavities can also be understood as the region between adjacent fins. Therefore, it is as important as the solid fin because both are found where augmentation and compactness of heat transfer are needed.

3.1 Isothermal Elemental Open Cavity

The search for best shapes starts studying the elemental open cavity or C-shaped cavity (Biserni et al. 2004). The flow system is shown in Fig. 1 and heat flows from the solid body to the ambient. The domain is assumed bidimensional for the sake of simplicity. There is uniform heat generation per unit of volume in the solid body

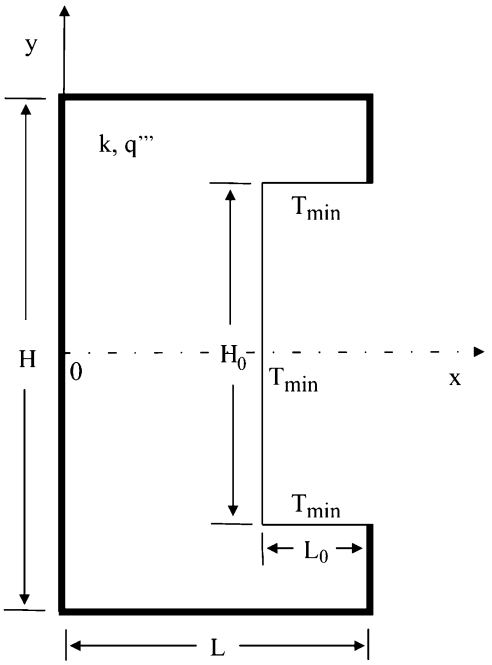

Fig. 1 Isothermal lateral intrusion into a two-dimensional conducting body with uniform heat generation

area, q''' (W/m^3). The solid body is isotropic and its thermal conductivity k (W/mK) is also uniform. The external surfaces of the solid body are insulated. The generated heat current ($q'''A$) is removed by the wall cavity which is isothermal at temperature $T_{\min}$. The performance indicator is the dimensionless maximal excess of temperature $\tilde{T}_{\max} = (T_{\max} - T_{\min})/(q'''A/k)$ which is proportional to the global thermal resistance $(T_{\max} - T_{\min})/(q'''A)$. The total area

$$A = HL \tag{6}$$

and the area of the cavity

$$A_0 = H_0 L_0 \tag{7}$$

are fixed. The shape of the body (external lengths L, H) and the shape of the cavity (H_0, L_0) are free to move and this change is allowed by the two degrees of freedom: H/L, the ratio between the height and the length of the solid body, and the H_0/L_0, the ratio between the height and the length of the cavity.

Equation 7 can be replaced by considering the fixed area fraction occupied by the cavity

$$\phi = \frac{A_0}{A} = \frac{H_0 L_0}{HL} \tag{8}$$

The search for best shapes starts by calculating the maximum temperature (hot spots) that occurs in the solid body and the location where it occurs. Changing the value of the degrees of freedom allows calculating the value of the global thermal resistance and discovers what shape has its minimum value. The conduction equation for the solid region is

$$\frac{\partial^2 \tilde{T}}{\partial \tilde{x}^2} + \frac{\partial^2 \tilde{T}}{\partial \tilde{y}^2} + 1 = 0 \tag{9}$$

where the dimensionless values are

$$\tilde{T} = \frac{T - T_{\min}}{q''' A/k} \tag{10}$$

$$\left(\tilde{x},\tilde{y},\tilde{H},\tilde{L},\tilde{H}_0,\tilde{L}_0\right) = \frac{x, y, H, L, H_0, L_0}{A^{1/2}} \tag{11}$$

The boundary conditions are given by the outer surfaces of the external body

$$\frac{\partial \tilde{T}}{\partial \tilde{x}} = 0 \text{ or } \frac{\partial \tilde{T}}{\partial \tilde{y}} = 0 \tag{12}$$

while the surfaces of the cavity are isothermal

$$\tilde{T} = 0 \tag{13}$$

This problem was solved numerically (Biserni et al. 2004) for several configurations (H/L, H_0/L_0, ϕ). Figure 2 shows that there is an optimal ratio H_0/L_0 which minimizes the global thermal resistance for several values of the area fraction for a fixed external aspect ratio ($H/L = 1$). The optimal cavity aspect ratio $(H_0/L_0)_{opt}$ increases and the minimal $\tilde{T}_{\max}$ decreases as the area fraction increases. This procedure was repeated for several values of the ratio H/L in Fig. 3. The results indicate that the minimal global thermal resistance decreases as H/L decreases and the area fraction also decreases. The same behavior of the optimal ratio $(H_0/L_0)_{opt}$ is also seen for the minimum global thermal resistance in Fig. 4. It is important to notice that Figs. 3 and 4 show that there is no optimal aspect ratio H/L. The results presented in Fig. 4 suggest that the results can be correlated as

$$\left(\frac{H_0}{L_0}\right)_{opt} \cong \phi \frac{H}{L} \tag{14}$$

The isothermal assumption considers that the heat transfer coefficient in the cavity surfaces is large enough; therefore, the thermal resistance imposed by the wall conduction is larger than the one by convection. If the cavity is bathed by a fluid

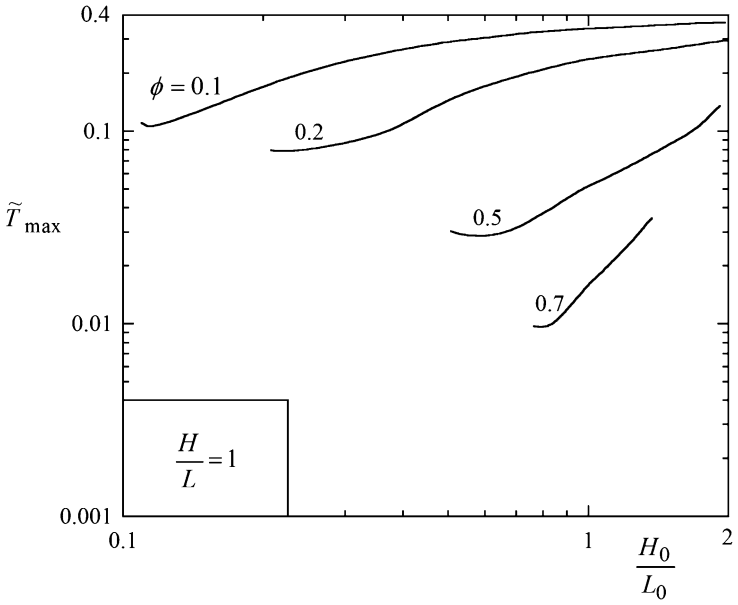

Fig. 2 The minimization of the global thermal resistance when the external shape of the heat generating body is fixed

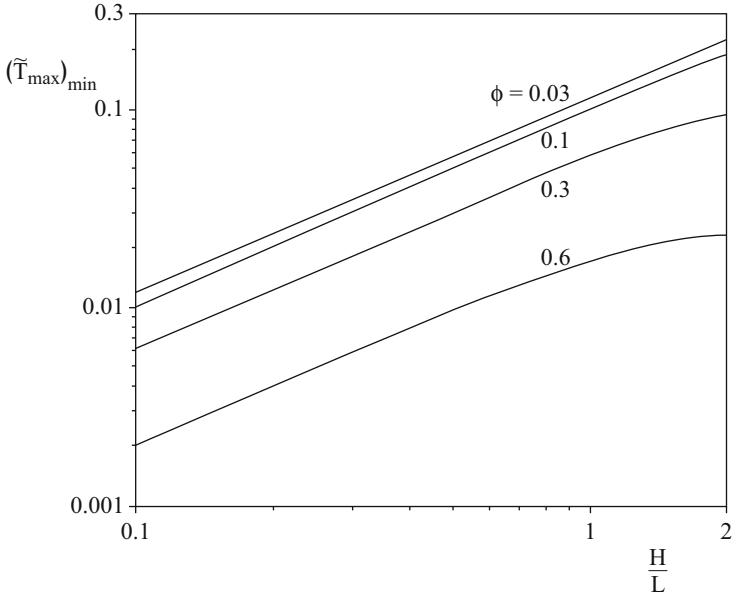

Fig. 3 The effect of the external shape H/L on the global thermal resistance minimized in Fig. 2

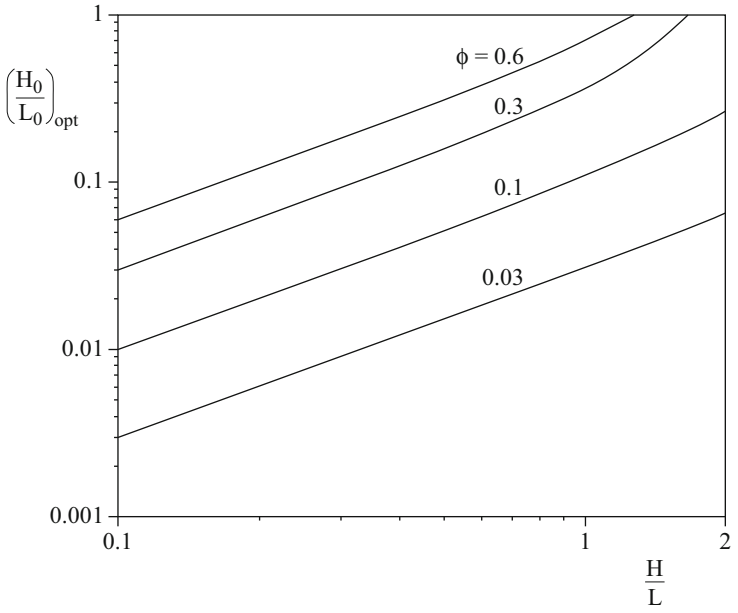

Fig. 4 The optimal shape of the cavity as function of H/L and ϕ

with a constant heat transfer coefficient, h, and constant temperature, T_∞, the boundary condition given by Eq. 13 is replaced by (Rocha et al. 2010)

$$-\frac{\partial \tilde{T}}{\partial \tilde{x}} = \lambda \tilde{T} \text{ or } -\frac{\partial \tilde{T}}{\partial \tilde{y}} = \lambda \tilde{T} \tag{15}$$

where the constant λ is defined as

$$\lambda = \frac{hA^{1/2}}{k} \tag{16}$$

Figure 5 shows that the behavior of the optimal cavity aspect ratio $(H_0/L_0)_{opt}$ and the minimal $\tilde{T}_{\max}$, as a function of the parameter ϕ, are similar to the ones obtained for the isothermal cavity when the parameter $\lambda = 0.005$. Figure 6 shows that the optimal aspect ratio $(H_0/L_0)_{opt}$ is almost insensitive to changes in the parameter λ in the range $0.1 < \lambda < 1$ for small ($\phi = 0.1$) or large ($\phi = 0.9$) values of the area fraction. However, for $\phi = 0.5$, the value of $(H_0/L_0)_{opt}$ can increase in approximately 20% from $\lambda = 0.1$ to $\lambda = 1$.

Figure 7 shows the effect of the external aspect ratio H/L on the optimal aspect ratio of the cavity for several area fractions when the parameter $\lambda = 0.005$. The optimal aspect ratio $(H_0/L_0)_{opt}$ increases as the external aspect ratio H/L increases. However, a change is noticed in the behavior of the $(H_0/L_0)_{opt}$ with respect to the area fraction: it increases when the area fraction increases in the range $0.1 < H/L < 2$;

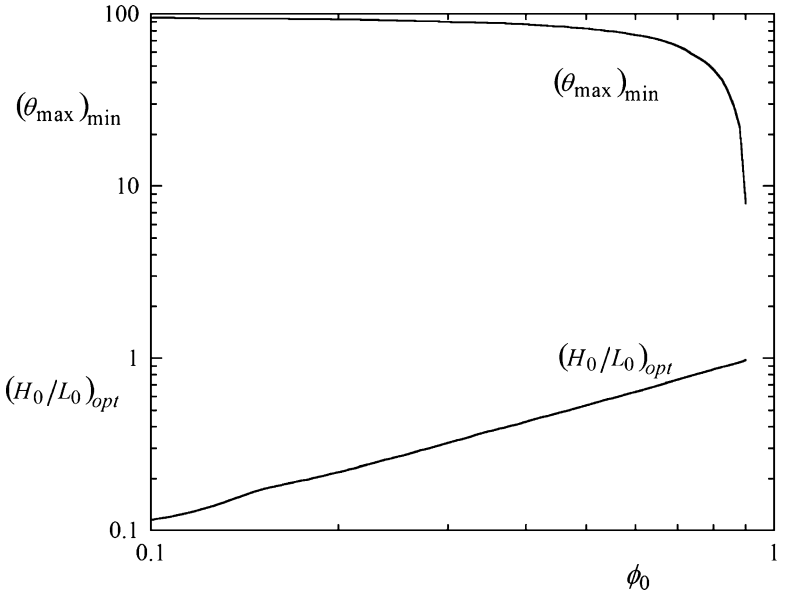

Fig. 5 The behavior of the best shapes and the dimensionless minimal maximal temperature as function of λ for $H/L = 1$

when the value of H/L is greater than 2, the value of $(H_0/L_0)_{opt}$ increases as the area fraction decreases.

3.2 Complex Cavities

The performance of the open cavity can be improved by giving it more freedom to morph. One way to do this is to increase the degrees of freedom of the open cavity, that is, to search for configurations which facilitate even more the flow of heat.

3.2.1 The First Construct: T-Shaped Cavity

The simplest first construct for the open cavity is the tree-shaped flow structure shown in the two-dimensional configuration of Fig. 8 (Biserni et al. 2004). This configuration is generated when the cavity assumes a bifurcated configuration, that is, the stem intrusion ($L_1 \times D_1$) branches into two elemental cavities ($L_0 \times D_0$) arranged as a T configuration. The total area which is given by Eq. 6 remains as a constraint. The solid material has the conductivity k and generates heat volumetrically at the uniform rate q'''. The problem is governed by Eq. 9. The surface of the cavity is isothermal at $T_{\min,}$ that is, the dimensionless boundary condition is given by Eq. 13, while the other surfaces are insulated (see Eq. 12). The indicator of performance is the dimensionless maximal excess of temperature which is also the global thermal resistance, $\tilde{T}_{\max} = (T_{\max} - T_{\min})/(q''' A/k)$. This configuration has

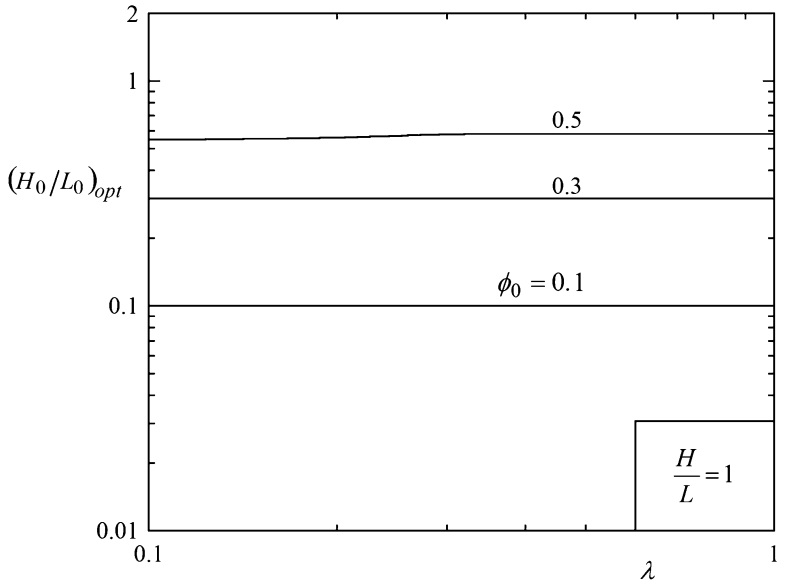

Fig. 6 The effect of the parameter λ in the optimal shape of the cavity for several values of the area fraction ϕ_0 and $H/L = 1$

two additional constrains, the area fraction occupied by the cavity in the plane of Fig. 8

$$\phi = \frac{2L_0D_0 + (L_1 - D_0/2)D_1}{HL} \tag{17}$$

and the area fraction occupied by the rectangle in which the T fits,

$$\psi = \frac{2L_0(L_1 + D_0/2)}{HL} \tag{18}$$

The configuration has three degrees of freedom that are represented by the ratios H/L, L_0/L_1 and D_0/D_1. It is assumed that $H/L = 1$ and the other two degrees of freedom were varied searching for better configurations, that is, configurations with the smaller $\tilde{T}_{\max}$ value. Firstly, L_0/L_1 was varied for a fixed value of D_0/D_1. Later, the process was repeated for several values of D_0/D_1.

Figure 9 shows that the results calculated for the optimal configurations with respect to L_0/L_1 are practically insensitive to changes in D_0/D_1. The effect of ϕ and ψ are shown in Figs. 10 and 11, respectively. The minimized global thermal resistance decreases as the ϕ and ψ increases, that is, the cavity becomes larger. The best geometries can be correlated when $H/L < 1$ by

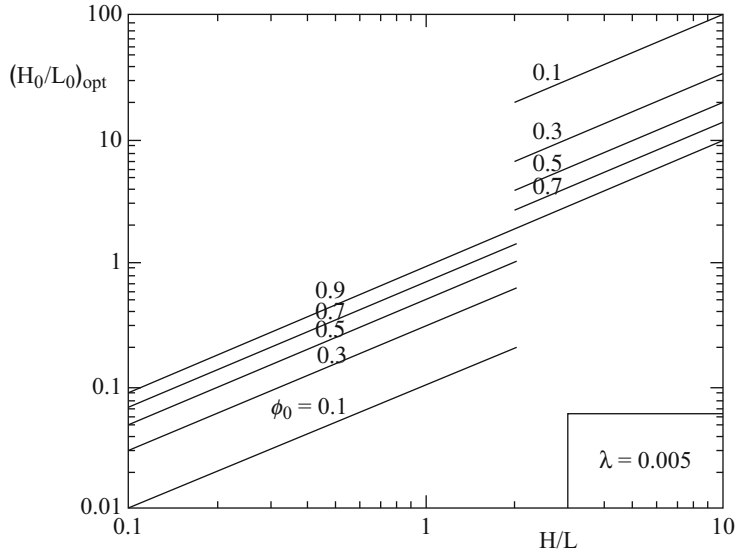

Fig. 7 The effect of the external aspect ratio H/L over the optimal aspect ratio of the cavity for several area fractions and $\lambda = 0.005$

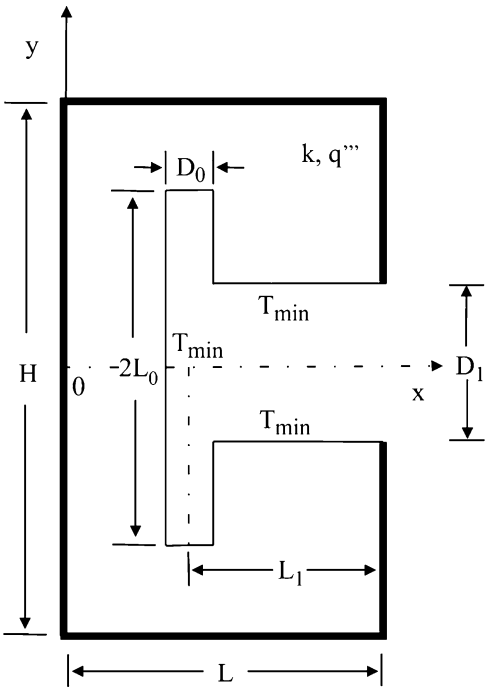

Fig. 8 T-cavity configuration: the first construct

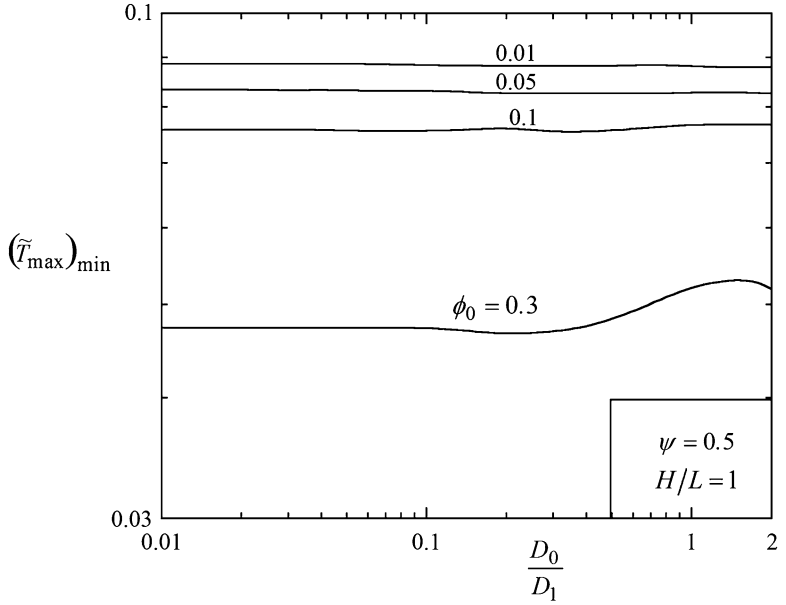

Fig. 9 The effect of the ratio D_0/D_1 on the minimized $(\tilde{T}_{\max})_{min}$ and the corresponding optimal ratio $(L_0/L_1)_{opt}$

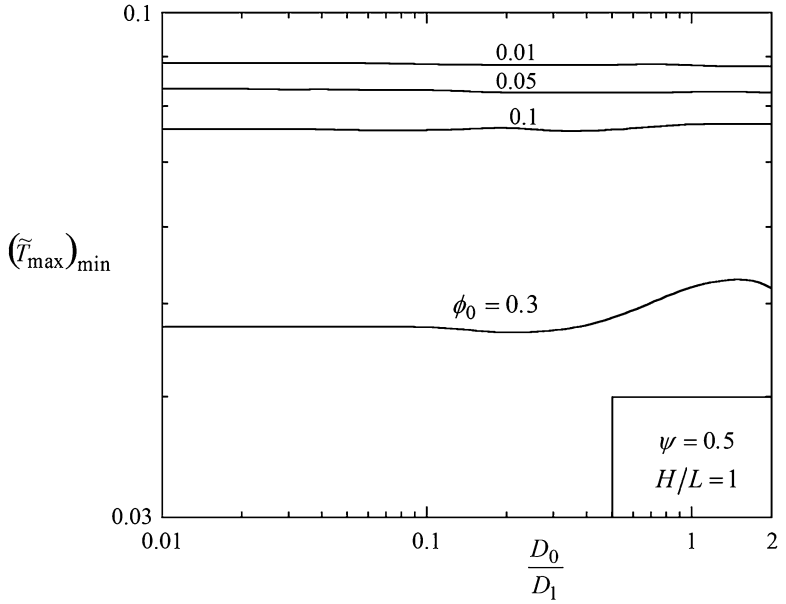

Fig. 10 The effect of the ratio $D_0/D1$ and ϕ_0 on the minimized global thermal resistance

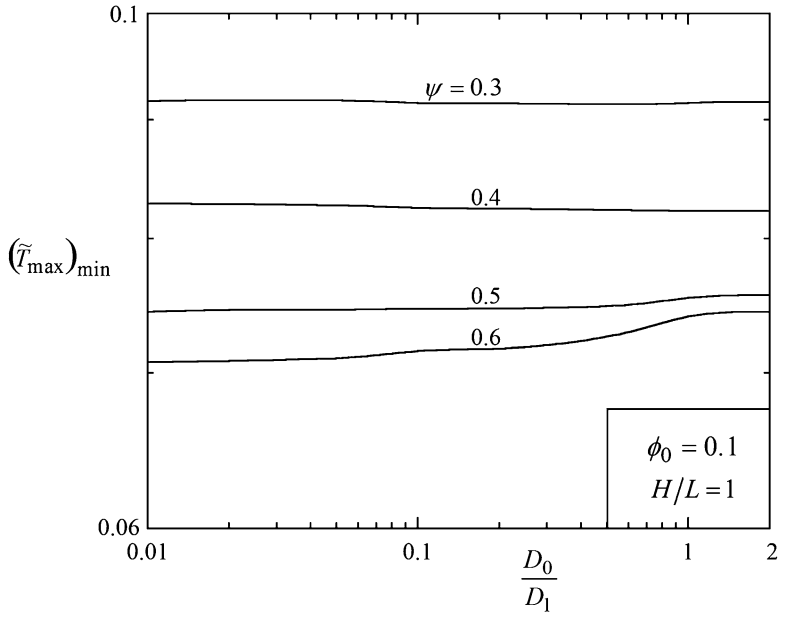

Fig. 11 The effect of ψ and D_0/D_1 on the minimized global thermal resistance

$$\frac{(H_0/L_0)_{opt}}{\phi H/L} \sim 1 \tag{19}$$

and

$$\left(\frac{L}{L_0}\right)^2 \sim 1 \tag{20}$$

When the performance of the elemental cavity shown in Fig. 1 is compared with the performance of the first construct drawn in Fig. 8, it is noted that the T-shaped cavity performs approximately 29% better under the same thermal conditions, uniform heat generation, and the same volume fraction $\phi = 0.1$.

The T-shaped open cavity was also studied when the cavity is bathed by a fluid with constant heat transfer coefficient, h, and constant temperature, T_∞ (Lorenzini et al. 2012a). The problem is the same as the one presented for the isothermal T-shaped cavity, except that the dimensionless temperature is given by

$$\theta = \frac{T - T_\infty}{q''' A/k} \tag{21}$$

and the boundary conditions on the surfaces of the cavity are given by a balance between the conduction and convection heat transfer,

$$-\frac{\partial\theta}{\partial\tilde{x}}=\frac{a^2}{2}\theta \text{ at } \tilde{x}=\left(\tilde{L}-\tilde{L}_0\right) \text{ and } -\frac{\tilde{H}_0}{2}\le\tilde{y}\le\frac{\tilde{H}_0}{2} \tag{22}$$

$$-\frac{\partial\theta}{\partial\tilde{y}}=\frac{a^2}{2}\theta \text{ at } \tilde{y}=-\frac{\tilde{H}_0}{2} \text{ or } \tilde{y}=\frac{\tilde{H}_0}{2} \text{ and}/\left(L-\tilde{L}_0\right)\le\tilde{x}\le\tilde{L} \tag{23}$$

where the parameter "a" which appears in Eqs. 22 and 23 was defined by Bejan and Almogbel (2000), as

$$a=\left(\frac{2hA^{1/2}}{k}\right)^{1/2}. \tag{24}$$

According to the new dimensionless temperature, the indicator of performance is

$$\theta_{\max}=\frac{T_{\max}-T_\infty}{q'''A/k}. \tag{25}$$

Figure 12 shows the results for several external shapes, H/L, when all the degrees of freedom shown in Fig. 8, L_0/L_1, H_0/L_0, and H_1/L_1, were investigated. The configuration with external shape $H/L = 1$ has the worst performance, that is, it presents the maximum value in the $\theta_{\max}$ curve shown in Fig. 12. However, all the configurations perform better when the cavities penetrate completely into the body

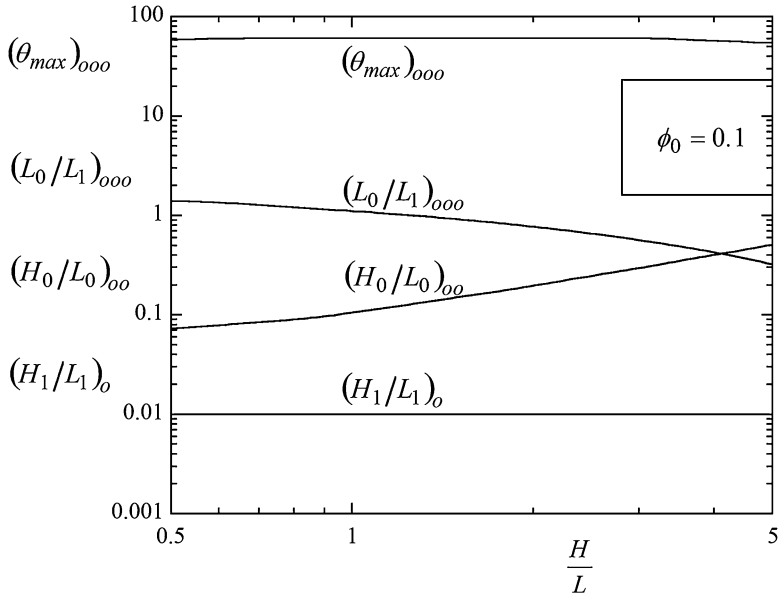

Fig. 12 The effect of the external shape H/L in the performance and geometry of the T-shaped cavity

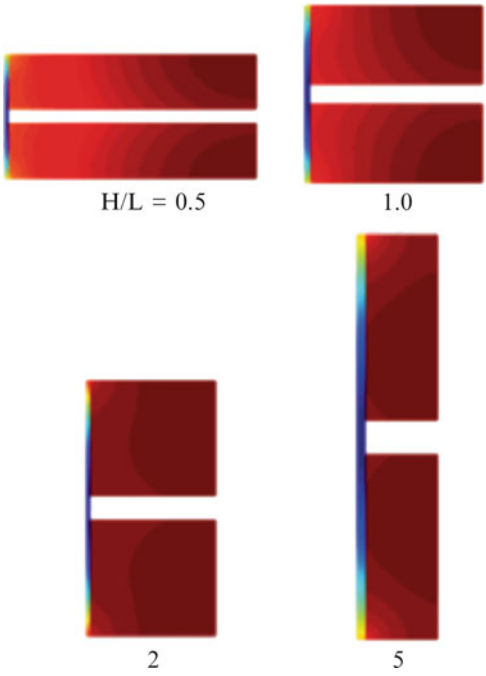

Fig. 13 The best shapes generated in Fig. 12

and the vertical branch of the T-shaped cavity occupies almost all the vertical length of the cavity. The body with an external shape $H/L = 5$ has the best performance in the studied range and it performs 23% better than the body with an external shape $H/L = 1$. The best shapes found in Fig. 12 are shown in scale in Fig. 13.

Lorenzini et al. (2013) studied the effect of the parameter "a," that is, the effect of the convective heat flux imposed at the cavity surfaces. Several values of parameter "a" (a = 0.1, 0.5, 1.0, and 2.0) were used to determine the effect of changing the flow conditions. The results indicate that there is no universal shape that is always better, that is, the T-shaped configuration morphs according to the convective flow in the cavity surfaces. If the value of "a" is small ($a = 0.1$), the best geometry is the one where the stem and the tributary branches have a higher penetration into the solid domain. As the value of "a" is increased, the best shapes migrate to the center of the body trying to distribute better the imperfections, that is, the hot spots regions, which increased from three ($a = 0.1$ and 0.5) to five ($a = 1$ and 2). The best shapes in scale are shown in Fig. 14.

3.2.2 Y-Shaped Cavity

The T-shaped configuration becomes a Y-shaped configuration if there is an angle, α, between the tributary branches and the horizontal axis as can be seen in Fig. 15 (Lorenzini et al. 2011). This creates an additional degree of freedom and gives more freedom to morph to the cavity. The mathematical model follows the one shown in the former section. However, Eqs. 17 and 18 are now replaced by

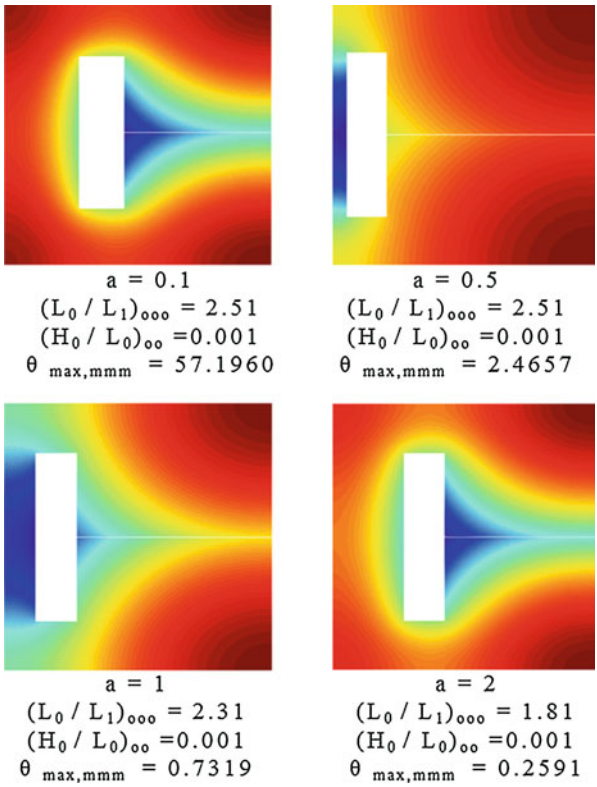

Fig. 14 The optimal shapes for several values of the parameter "a"

$$\phi_c = \tilde{L}_1\tilde{t}_1 + 2\tilde{L}_0\tilde{t}_0 + \tilde{t}_1\tilde{t}_0 \quad \cos\alpha - \tilde{t}_0^2 \quad \sin\alpha\cos\alpha \tag{26}$$

$$\psi = \left(\tilde{L}_1 + \tilde{L}_0 \quad \sin\alpha + \tilde{t}_0 \quad \cos\alpha\right)\left(2\tilde{L}_0 \quad \cos\alpha + \tilde{t}_1\right) \tag{27}$$

To begin with, the surface of the cavity is isothermal ($\theta = 0$) and the other surfaces are adiabatic. The indicator of performance is defined as $\theta_{\max} = (T_{\max} - T_{\min})/(q''' A/k)$. The search for better and better shapes is the same as the one adopted in the former section. The configuration shown in Fig. 15 has four degrees of freedom: H/L, t_1/t_0, L_1/L_0, and α. The first parameter to be studied is the tributary angle, α, between the bifurcated branch and the horizontal axis. Figure 16a shows that there is an optimal α angle that minimizes $\theta_{\max}$ for several values of the degree of freedom L_1/L_0 when the other parameters and degrees are fixed.

The procedure used in Fig. 16a is now repeated for several values of the third degree of freedom t_1/t_0. The results are summarized in Fig. 16b where the minimized maximal temperature $(\theta_{\max})_m$ is shown as function of the ratio L_1/L_0 for several ratios t_1/t_0 Figure 16c summarizes the procedure of Fig. 16a, b for the study of the third degree of freedom t_1/t_0 This figure shows that the value of $t_1/t_0 = 11.0$ minimized the global thermal resistance. The corresponding values for the other

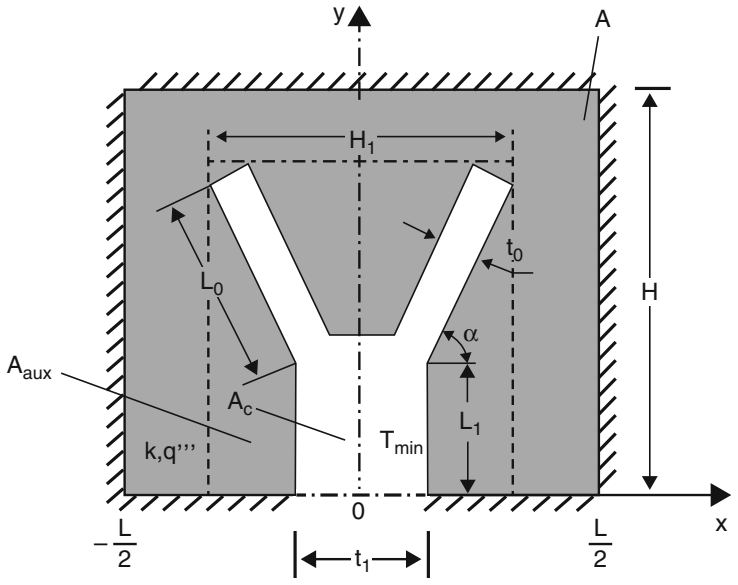

Fig. 15 Y-shaped cavity into a two-dimensional conducting body with uniform heat generation

degrees of freedom are $\alpha_{oo} = 1.55$ and $(L_1/L_0)_o = 0.007$. The last degree of freedom, H/L, is investigated in Fig. 16d. The results show that the global thermal resistance decreases as the ratio H/L increases. The values of the minimum global thermal resistance as function of all the four degrees of freedom are correlated by

$$(\theta_{\max})_{mmm} = 0.42(H/L)^{-2.66}(t_1/t_0)_o^{0.3}(L_1/L_0)_{oo}^{0.59}\alpha_{ooo}^{0.66} \tag{28}$$

Equation 28 is valid in the range: $0.5 \le H/L \le 5$, $2 \le (t_1/t_0)_o \le 55$, $0.007 \le (L_1/L_0)_{oo} \le 0.6$, and $0.001 \le \alpha_{ooo} \le 1.57$.

3.2.3 Second Construct (H-Shaped Cavity)

Assembling together two T-shaped cavities (the first construct) gives us the second construct (Biserni et al. 2007) or H-shaped cavity shown in Fig. 17. The cavity is isothermal, and therefore the mathematical model is the same as the one used in the former section, except that the area fraction of the cavity is given by

$$\phi = 4\tilde{H}_0\tilde{L}_0 + 2\tilde{H}_1\tilde{L}_1 + \tilde{H}_2\tilde{L}_2 \tag{29}$$

The area fraction ψ (see Eq. 18) is not used here; therefore, the H-shaped cavity has five degrees of freedom: L_0/L_2, L_1/L_2, H_0/H_2, H_0/H_2, and H_2/H_2. The aspect ratio H/L is fixed ($H/L = 1$). The search for better configurations consists of investigating the effect of all the five degrees of freedom. The results are correlated as

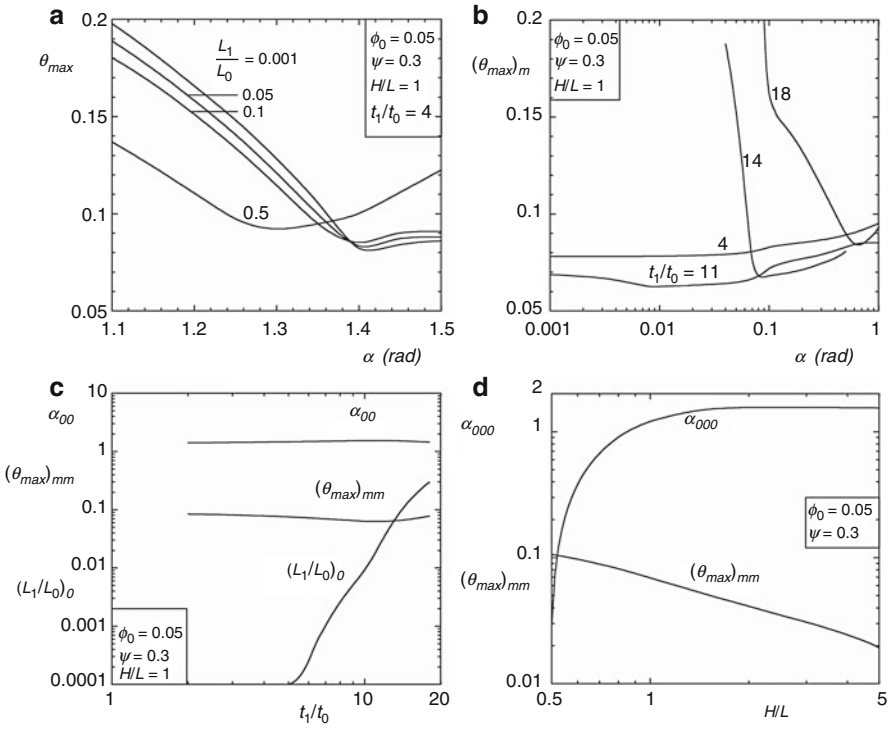

Fig. 16 The sequence of the steps used to search for the best shapes of Fig. 15

$$\left(\tilde{T}_{\max}\right)_{mmmm} = 0.02\left(\frac{H_2}{L_2}\right)^{-0.13}\left(\frac{L_0}{L_2}\right)_{oo}^{0.27}\left(\frac{L_1}{L_2}\right)_{o}^{0.1}\left(\frac{H_0}{H_2}\right)_{oooo}^{-0.13}\left(\frac{H_1}{H_2}\right)_{ooo}^{-0.0043} \tag{30}$$

$$\frac{H_2}{L_2} = 0.048\left(\frac{H_0}{H_2}\right)_{oooo}^{-0.78}\left(\frac{H_1}{H_2}\right)_{ooo}^{-0.11} \tag{31}$$

$$\left(\frac{L_0}{L_2}\right)_{oo} = 1.44\left(\frac{L_1}{L_2}\right)_{o}^{0.53} \tag{32}$$

3.2.4 Giving Freedom to Morph

Examples of several configurations have been studied so far. It has been shown that when giving freedom to the system to morph, that is, facilitating the access of its currents, the performance of the system improves. This idea is presented for isothermal cavities in Fig. 18 ($\phi = 0.05$, $H/L = 1$). This figure shows that the global thermal resistance decreases as the configuration has more degrees of freedom. The X-shaped cavity (Fig. 18e, Lorenzini et al. 2014b) performs approximately 70% better than the elemental cavity (Fig. 18a). The X-shaped cavity (Fig. 18f) was also

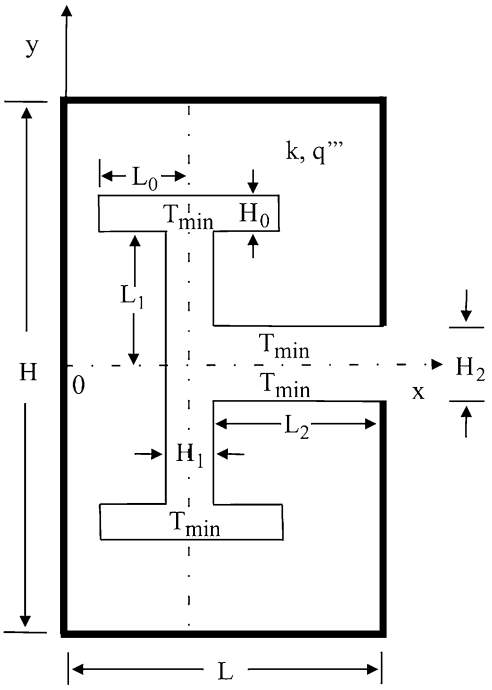

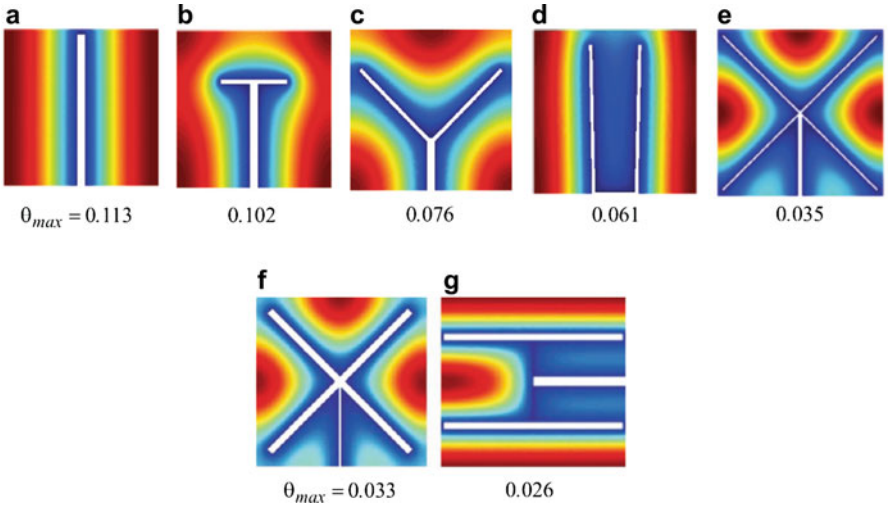

Fig. 17 Isothermal H-shaped intrusion into a two-dimensional conducting body with uniform heat generation

Fig. 18 Evolution of isothermal cavities

compared to the second construct, the H-shaped cavity (Fig. 18f) keeping $\phi = 0.1$, $H/L = 1$. The results show that the global thermal resistance for the second construct is 21% smaller than the one calculated for the X-shaped cavity.

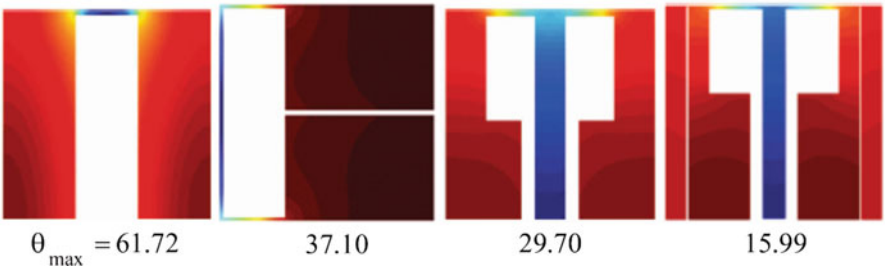

Fig. 19 Evolution of convective cavities ($\phi = 0.3$)

Figure 19 illustrates the evolution of the cavities that are bathed by a fluid with a constant heat transfer coefficient, h, and a constant temperature, T_∞. The results show that the performance improves approximately by 74% from the elemental cavity to the more complex cavity: a T-Y-shaped cavity with two additional lateral intrusions (Lorenzini et al. 2012b) cooled by convection when the area fraction is set $\phi = 0.3$.

4 Flow Spacings

Natural tree-shaped networks are the best flowing routes between one point and an area (or volume) because they bathe the available space with channels of multiple scales, which are allocated optimally to interstitial areas (or volumes). Many scales are organized hierarchically – few are large, many are small – and are distributed nonuniformly. They are positioned in the right places. Optimal bathing, optimal packing, and maximum density of function come from the drawing that consists of multiple scales that are arranged nonuniformly.

An example of flow spacings (Da Silva et al. 2004a) is shown in Fig. 20, where the best way to arrange a number of heat generating components (q', D_0) on a wall cooled by laminar forced convection is a nonuniform, multiscale arrangement. The spacings (S_i) must be smaller upstream and larger downstream, and must be zero in a region (x_0) near the tip of the boundary layer. Multiscale architectures were also obtained for cooling by natural convection (Da Silva et al. 2004b) and for walls with heat sources of finite thickness (Da Silva et al. 2005). The architectures of Fig. 20 stand in contrast with current designs of cooled electronics, where heat-generating components of equal strength are arranged equidistantly on a substrate.

5 Trees for Heat Conduction

In the cooling of electronics, the frontier is being pushed in the direction of smaller dimensions and greater svelteness (see Bejan and Lorente 2008). There comes a point where miniaturization makes convection cooling impractical, because the fluid

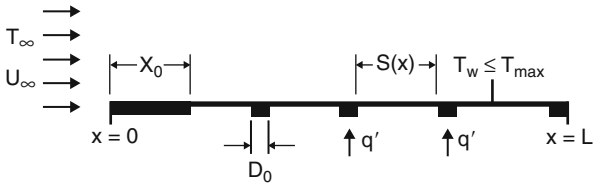

Fig. 20 Multiple length scales on a wall with concentrated heat sources and maximum heat transfer density in laminar forced convection (Da Silva et al. 2004a)

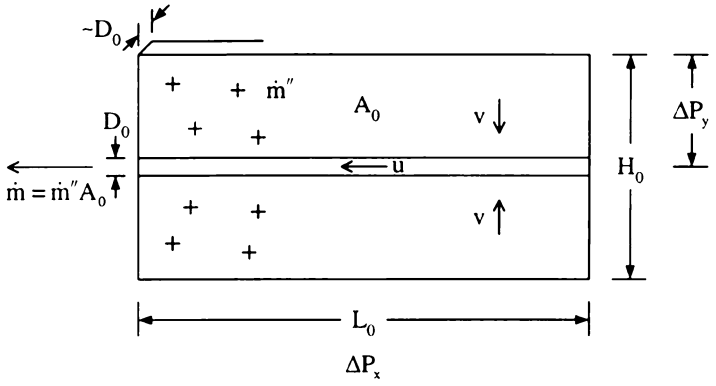

Fig. 21 Elemental area of a river basin viewed from above: seepage with high resistivity Darcy flow proceeds vertically, and channel flow with low resistivity proceeds horizontally. Rain falls uniformly over the rectangular area $A_0 = H_0/L_0$. The flow from the area to the point sink encounters minimum global resistance when the external shape H_0/L_0 is optimized. The generation of geometry is the mechanism by which the area-point flow system assures its persistence in time, its survival

channels would take too much space. In this limit, the only way to vehicle the heat out of the package is by conduction. From this argument came the proposal (Bejan 1996a) to cool heat-generating volumes by using tree-shaped inserts of high-conductivity blades and fibers.

Trees for conduction cooling are now a growing literature (e.g., Lewins 2003; Neagu and Bejan 2001; Vargas and Bejan 2002; Blyth and Pozrikidis 2003; Wechsatol et al. 2001, 2002a, b, 2005a, b; Lorente et al. 2002; Gosselin and Bejan 2005; Brod 2003; Tondeur and Luo 2004; Gosselin 2005; Pence 2002). The first conduction trees were generated by using the construction method illustrated in Figs. 21 and 22. At the elemental level in Fig. 21, the rectangle $H_0 \times L_0$ is a low-conductivity (k_0) material that generates heat volumetrically and uniformly q''' (W/m^3). A blade of constant thickness (D_0) and high conductivity k_p is inserted along the longest of the two axes of the rectangle. The sink (T_0) is the left end of the k_p blades. The hot spots (T_{max}) occur in the two right-hand corners of the rectangle. The total heat current is $q' = q''' H_0 L_0$. The size $H_0 L_0$ is fixed, but the shape (H_0 / L_0) may vary. The elemental thermal resistance $(T_{max} - T_0)/q'$ is minimum when

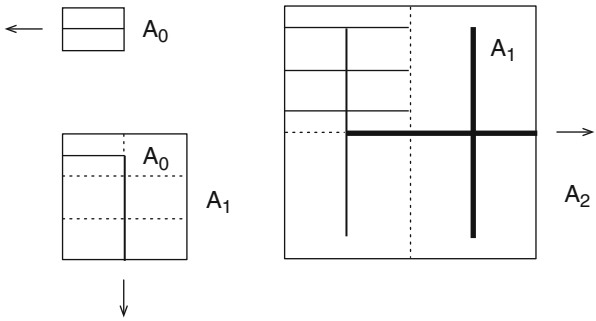

Fig. 22 Constructal sequence of assembly and optimization, from the optimized elemental area A_0 (Fig. 21) to progressively larger area-point flows (Bejan 1997)

$$H_0/L_0 = \left(k_0 H_0/k_p D_0\right)^{1/2} \tag{33}$$

The generation of the tree continued at large scales, by assembling optimal numbers of smaller constructs into larger constructs (e.g., Fig. 22).

A better tree performance is obtained by endowing the flow configuration with more freedom to morph (Bejan and Lorente 2004, 2005). Ledezma et al. (1997) used a fully numerical approach in which they replaced the construction sequence of Fig. 22 with numerical simulations of conduction in the composite domain (k_0, k_p), with the freedom to vary all the geometric features of the emerging tree structure. First, they abandoned the assumption that the high-conductivity insert is a blade of constant thickness. As shown in the second frame of Fig. 23, the optimal profile of the k_p insert is such that D_0 increases as $x^{1/2}$, where x is measured away from the tip. Relative to the design of Eq. 33, the decrease in the global thermal resistance of the elemental volume is 6%. Even greater reductions in global thermal resistance result from discarding the assumption that the element is rectangular (Neagu and Bejan 2001). The bottom frame of Fig. 23 shows that there is an optimal leaflike elemental shape, as there is an optimal shape for the k_p fiber. Increasing the freedom to morph the structure leads to higher performance levels and to designs that look more natural.

The assumption that the k_p branches are perpendicular to their stems was also abandoned (Ledezma et al. 1997). For example, in a first construct with $\tilde{k} = k_p/k_0 = 50$ and $\phi_1 = V_{p1}/V = 0.1$, it was found that the optimal angle is such that the branch deviates from the perpendicular by 4° and that in this refined geometry the global resistance is smaller by 5.8% than before. Angled branches increase the global performance and make the tree architecture look more natural.

Ledezma et al. (1997) also abandoned the sequential construction of larger assemblies and in a composite domain such as Fig. 24 optimized the numbers and positions of every high-conductivity insert. There are three k_p-blade thicknesses, $D_0 < D_1 < D_2$. Because of the increased freedom, the numerical formulation made it possible to omit the thin (D_0) branches that would have crowded the stem (D_2). Figure 24 was drawn for $\tilde{k} = k_p/k_0 = 300$, $\phi_2 = V_{p2}/V = 0.1$, $D_1/D_0 = 5$, $D_2/D_1 = 2$, and eight D_0 blades on one D_1 blade. The purpose of this figure is to illustrate the effect that the number (n_2) of D_1 blades has on the global performance.

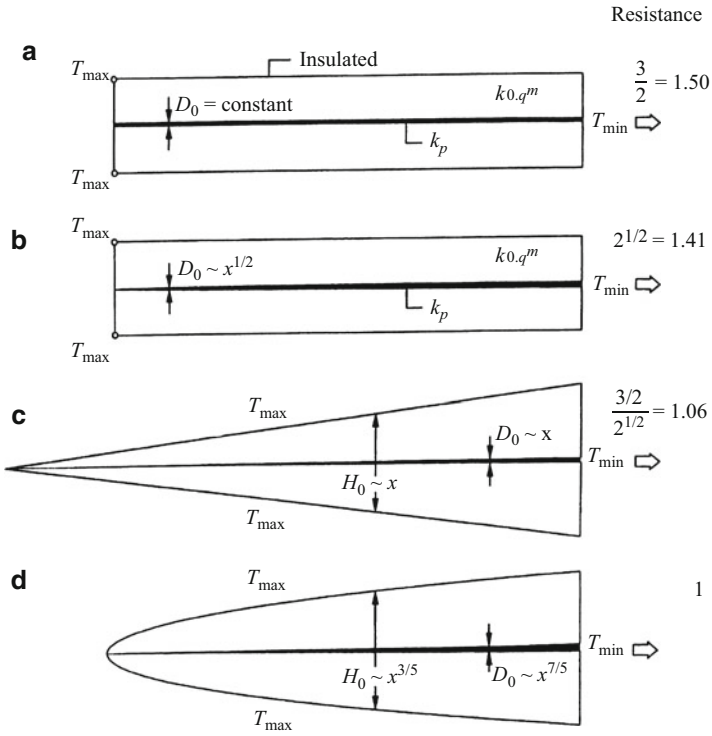

Fig. 23 Elemental conduction volume with progressively greater freedom to morph and progressively higher performance (Neagu and Bejan 2001)

From (a) to (c), the dimensionless global thermal resistance $\Delta T_2 k_0/q''' A_2$ takes the values 0.0379, 0.0354, and 0.0374, where A_2 is the total size of the rectangular domain and ΔT_2 is the temperature difference between the hot spot (the left corners) and the heat sink (midpoint of the right side). The competing designs in Fig. 24 show that the best is (b), where the number of D_1 inserts is $n_2 = 4$. This result differs from the simplest approach (Bejan 1996b), in which the rule of assembly was pairing dichotomy, that is, $n_2 = 2$. The result that $n_2 = 4$ coincides with the optimal construction rule found for river drainage.

Figure 24 also shows that the performance of designs (a) and (c) is not too far from that of design (b). This means that tree-shaped flow architectures that have been optimized partially or completely are *robust*. By using the results tabulated in Bejan (1997), one can show that the analytical construction sequence produces a structure with a global resistance ($\Delta T_2 k_0/q''' A_2$) of the same order of magnitude as in Fig. 24, but larger. This comparison shows the approximate character of the simplest approach and the merits of increasing the number of degrees of freedom of the structure simulated numerically.

In drawings such as Figs. 22 and 24, tree patterns that maximize flow access are discovered. Every detail of the tree geometry is the result of invoking the Constructal

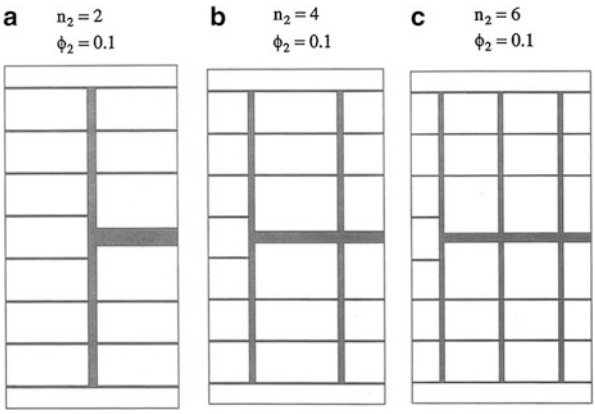

Fig. 24 Second construct optimized numerically, and the effect of changing the number n_2 of high-conductivity inserts of intermediate size D_1 (Ledezma et al.1997)

Table 1 How the balancing of high resistivity flow with low resistivity flow in a wide diversity of flow systems (courtesy of Stéphen Périn)

		How	
Application	What	Interstices (high resistance at the smallest fixed scale)	Channels (low resistance at larger scales)
Electronics packages	Heat	Low-conductivity substrate	High-conductivity inserts (blades, needles)
River basins	Water	Darcy flow through porous media	Rivulets and rivers
Lungs	Air	Diffusion in alveoli, tissues	Bronchial passages
Circulatory systems	Blood	Diffusion in capillaries, tissues	Blood vessels, capillaries, arteries, veins
Turbulent flow	Momentum	Laminar, viscous diffusion	Streams, eddies
Urban traffic	People	Walking in urban structure	Street traffic
Economics	Goods	Hand delivery and collection	Freight, rail, truck, air, ship

Law. The discovery of the tree as the flow architecture for maximal access between one point and an infinity of points is general – it is not restricted to trees of streets (Bejan 1996a) and trees of high-conductivity inserts (Bejan 1996a). The generality of the tree discovery is stressed by Table 1, which shows that "how" unites and "what" divides. How the tree is generated (through a balance between high resistivity and low resistivity) is the same in many classes of flow systems, regardless of the diversity of the currents that flow through them. To see the principle that unites is harder than to see the "diversity" of flow systems in nature and engineering.

A related direction of progress on multiscale structures for conduction is the development of optimal rough surfaces for minimal thermal contact resistance (Neagu and Bejan 2001; Vargas and Bejan 2002; Blyth and Pozrikidis 2003).

6 Constructal Invasion of a Conducting Tree into a Conducting Body

The Constructal Law statement is general. It does not use words such as complex versus simple or natural versus engineered. There are several classes of flow configurations in nature, and each class can be derived from the Constructal Law in several ways: analytically or numerically, approximately or more accurately, blindly (random search) or using strategy (shortcuts), and so on. Classes that have been treated in detail, and by several methods, are the cross-sectional shapes of ducts, the cross-sectional shapes of rivers, internal spacings, and tree-shaped architectures.

Regarding the tree architectures, they are treated not as models but as fundamental problems of access to flow: volume to point, area to point, line to point, and the respective reverse flow directions. Important is the geometric notion that the "volume," the "area," and the "line" represent infinities of points.

The theoretical discovery of trees stems from the decision to connect one point (source or sink) with an infinity of points (volume, area, line). It is the reality of the continuum (the infinity of points) that is routinely discarded by modelers who approximate the space with a finite number of discrete points and then cover the space with drawings made of sticks, which cover the space incompletely (and from this, fractal geometry). The reality of the continuum requires a study of the interstitial spaces between the tree links. The interstices can only be bathed by high-resistivity diffusion (an invisible, disorganized flow), whereas the tree links serve as conduits for low-resistivity organized flow (visible streams, ducts).

The two modes of flowing with imperfection (irreversibility), the interstices and the links, must be balanced so that together they ease the global flow. The flow architecture is the graphical expression of the balance between channels and their interstices. The deduced architecture (tree, duct shape, spacing, etc.) is the distribution of imperfection over the available flow space. It is the architecture for access into and out of the flow space, which is finite. Those who model natural trees and then draw them as black lines on white paper (while not struggling to discover the layout of every black line on its allocated white patch) miss half of the drawing. The white is as important as the black.

The Constructal-Law discovery of tree-shaped flow architectures was based on three approaches. It started in 1996 with an analytical shortcut (Bejan 1996a, 1997) based on several simplifying assumptions: 90 angles between stem and tributaries, a construction sequence in which smaller optimized constructs are retained, constant-thickness branches, and so on. Months later, the same problem was solved numerically (Ledezma et al. 1997) by abandoning most of the simplifying assumptions (e.g., the construction sequence) used in the first papers. In 1998, we reconsidered the problem in an area-point flow domain with randomly moving low-resistivity blocks embedded in a high-resistivity background (Errera and Bejan 1997; Bejan 2000) with Darcy flow (permeability instead of conductivity and resistivity). Along the way, we found better performance and trees that look more "natural" as we progressed in time, that is, as we endowed the flow structure with more freedom to morph.

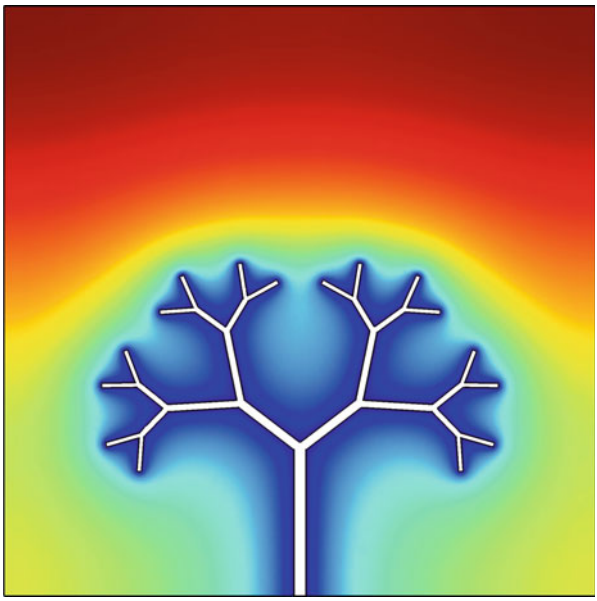

Fig. 25 Constructal invasion of a conducting tree into a conducting body

Figure 25 shows a recent tree design for conduction in a heat generating medium with high-conductivity channels that are the most free to morph (Kobayashi et al. 2013). Darcy fluid flow is one form of "diffusion," that is, the same physics phenomenon as thermal diffusion (Fourier conduction) and electrical diffusion (Ohm conduction).

7 The Effect of Size on the Design of Distributed Heating on the Landscape

The global flow system is a tapestry of nodes of production embedded in areas populated by users and environment, distributing and collecting flow systems, all linked, and sweeping the earth with their movement. Constructal theory and design (Bejan and Lorente 2008) are showing that the whole basin is flowing better (with fewer obstacles globally) when the production nodes and the channels are allocated in certain ways to the covered areas (the environment). This is how the inhabited globe becomes a live system – a living tissue – and why its best future can be designed based on principle. With the Constructal Law, this design can be pursued predictively.

The landscape emerges as a tapestry of nodes of production and lines of distribution. The nodes are few and large, and the branches that reach the users are many and small. It has also been discovered that this tapestry must be woven according to a vascular design that depends on the size of the whole system. For example, while distributing heated water from a central heater to a square area with N uniformly distributed users, the flow architecture can be radial (r), dichotomous (2), or a construct (4) based on a quadrupling rule, Fig. 26. The lower part of the figure

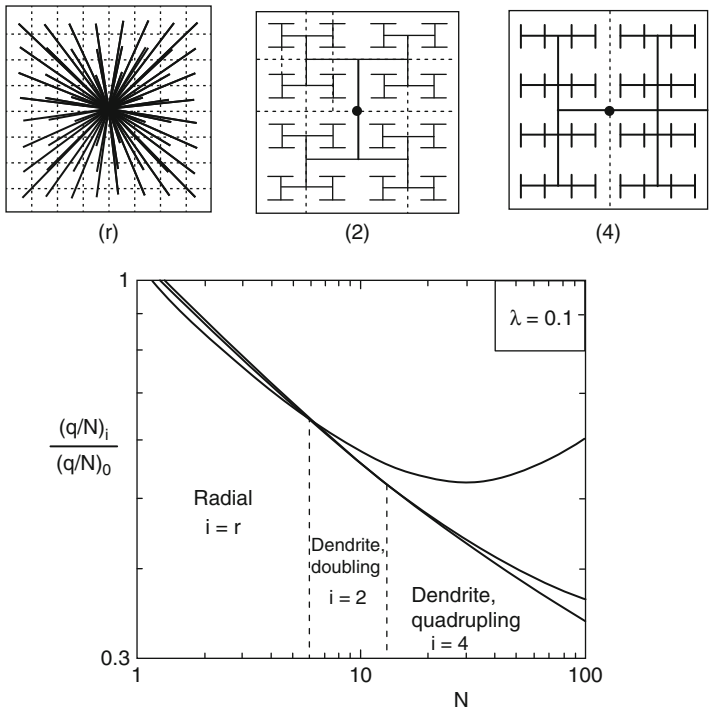

Fig. 26 The effect of size on the design of distributed heating on the landscape. The total heat loss per user decreases as the size of the inhabited area increases. The heat loss per user is lower when the architecture evolves step-wise from radial to dendritic as N increases

shows that the total heat loss per user (i.e., the loss at the center and along the distribution lines) decreases as the size of the landscape (N) increases. In the pursuit of efficiency (less fuel required per user), the flow architecture must change stepwise from (r) to (2), and finally to (4) as the overall size increases.

8 Conclusions

The fast growth of the Constructal-Law field, which is documented in this chapter is an illustration of the much broader phenomenon of how and why science evolves and improves. Science is an evolutionary design in which what we know – what is true, what works – becomes simpler, more accessible, and easier to teach (Bejan 2009).

The Constructal Law is a new law of physics that broadens significantly the reach of thermodynamics (Bejan and Lorente 2004). The merger of mechanics with caloric theory into thermodynamics in 1851 was not the end of this morphing by simplification and replacement. The caloric line continued to this day as thermometry, calorimetry, and heat transfer (Fig. 27). Although mechanics and caloric theory were

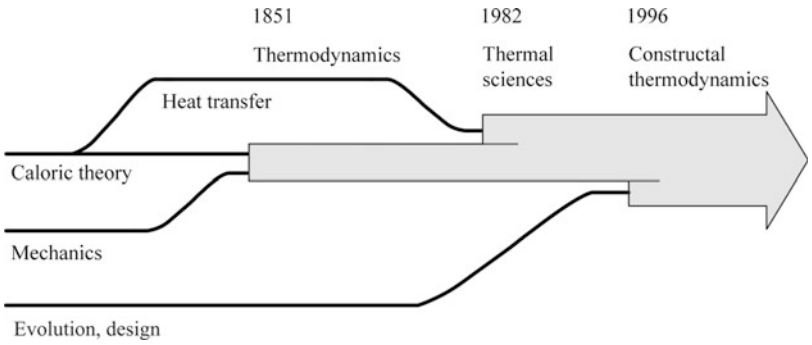

Fig. 27 The evolution and spreading of thermodynamics during the past two centuries (After Bejan 1982, Diagram 1, p. viii)

incorporated in thermodynamics, heat transfer developed into a self-standing discipline, with major impact on applied mathematics, fluid mechanics, and aerodynamics. Still, its proper place is in thermodynamics along with all the other caloric teachings.

The merger of heat transfer with thermodynamics was predicted in 1982 in the preface of Bejan (1982) (Fig. 27), and the prediction came true in the two decades that followed. Heat transfer journals became journals of "thermal sciences" (which means heat transfer and thermodynamics), and in many universities the heat transfer and thermodynamics courses were combined into a single course on thermal sciences.

Thermal sciences expanded in new directions, most vigorously now because of the Constructal Law, which unifies science (physics, biology, engineering, social sciences). Constructal thermodynamics (Bejan and Lorente 2004) places the concepts of life, design, and evolution in physics. It constitutes a wide open door to new advances, especially in areas where design evolution is key to performance, for example, in logistics (Birla 2005), biological evolution (McGhee 2011), art (Burstein 2011), and business and economics (Hwang and Horowitt 2012).

Constructal thermodynamics claims a role for design, configuration, and geometry in understanding the language of nature (Dellian 2012). The Constructal Law runs against reductionism and empowers the mind to see the whole, its design, performance, and future (Bejan and Zane 2012; Bejan 2016). In modern times, physics grew on a course tailored to infinitesimal effects. The Constructal Law is a jolt the other way, a means to rationalize macroscopic design, objective, and behavior (Bejan 2000).

9 Cross-References

► Design of Thermal Systems
► Numerical Methods for Conduction-Type Phenomena

Acknowledgments Prof. Bejan's work was supported by a grant from the National Science Foundation. Prof. Rocha thanks the support of CNPq, Brasília, DF, Brazil.

References

Bejan A (1982) Entropy generation through heat and fluid flow. Wiley, New York

Bejan A (1993) Heat transfer. Wiley, New York

Bejan A (1996a) Constructal-theory network of conducting paths for cooling a heat generating volume. Int J Heat Mass Transf 40:799–816. Published on 1 Nov 1996

Bejan A (1996b) Entropy generation minimization. CRC Press, Boca Raton

Bejan A (1996c) Street network theory of organization in nature. J Adv Transp 30(2):85–107

Bejan A (1997) Advanced engineering thermodynamics, 2nd edn. Wiley, New York

Bejan A (2000) Shape and structure from engineering to nature. Cambridge University Press, Cambridge, UK

Bejan A (2009) Science and technology as evolving flow architectures. Int J Energy Res 33:112–125

Bejan A (2012) Interviewed by Kosner AW "Freedom is good for design", How to use Constructal Theory to liberate any flow system. Forbes, 18 Mar 2012

Bejan A (2016) The physics of life: the evolution of everything. St. Martins's Press, New York

Bejan A, Almogbel M (2000) Constructal T-shaped fins. Int J Heat Mass Transf 43 (12–15):2101–2115

Bejan A, Lorente S (2004) The constructal law and the thermodynamics of flow systems with configuration. Int J Heat Mass Transf 47:3203–3214

Bejan A, Lorente S (2005) La Loi Constructale. L'Harmattan, Paris

Bejan A, Lorente S (2008) Design with constructal theory. Wiley, Hoboken

Bejan A, Zane JP (2012) Design in nature: how the constructal law governs evolution in biology, physics, technology, and social organization. Randon House LLC/Doubleday, New York

Birla M (2005) FedEx delivers: how the world's leading shipping company keeps innovating and outperforming the competition. Wiley, Hoboken

Biserni C, Rocha LAO, Bejan A (2004) Inverted fins: geometric optimization of the intrusion into a conducting wall. Int J Heat Mass Transf 47:2577–2586

Biserni C, Rocha LAO, Stanescu G, Lorenzini E (2007) Constructal H-shaped cavities according to Bejan's theory. Int J Heat Mass Transf 50:2132–2138

Blyth MG, Pozrikidis C (2003) Heat conduction across irregular and fractal-like surfaces. Int J Heat Mass Transf 46:1329–1339

Brod H (2003) Residence time optimised choice of tube diameters and slit heights in distribution systems for non-Newtonian liquids. J Non-Newtonian Fluid Mech 111:107–125

Burstein J (2011) Spark: how creativity works. Harper, New York

Da Silva AK, Lorente S, Bejan A (2004a) Optimal distribution of discrete heat sources on a plate with laminar forced convection. Int J Heat Mass Transf 47:2139–2148

Da Silva AK, Lorente S, Bejan A (2004b) Optimal distribution of discrete heat sources on a wall with natural convection. Int J Heat Mass Transf 47:203–214

Da Silva AK, Lorente S, Bejan A (2005) Constructal multi-scale structures with asymmetric heat sources of finite thickness. Int J Heat Mass Transf 48:2662–2672

Dellian E (2012) The language of nature is not algebra. Neutonus Reformatus, Paper no. 40. http://www.neutonus-reformatus.de/download/dellian_the_language_of_nature_is_not_algebra.pdf. Accessed 15 Dec 2016

Errera MR, Bejan A (1997) Deterministic tree networks for river drainage basins. Fractals 6:245–261

Gosselin L (2005) Minimum pumping power fluid tree networks without a priori flow regime assumption. Int J Heat Mass Transf 48:2159–2171

Gosselin L, Bejan A (2005) Emergence of asymmetry in constructal tree flow networks. J Appl Phys 98:104903

Hwang VW, Horowitt G (2012) The rainforest: the secret to building the next silicon valley. Regenwald, Los Altos Hills

Kobayashi H, Lorente S, Anderson R, Bejan A (2013) Trees and serpentines in a conducting body. Int J Heat Mass Transf 56:488–494

Ledezma GA, Bejan A, Errera MR (1997) Constructal tree networks for heat transfer. J Appl Phys 82:89

Lewins J (2003) Bejan's constructal theory of equal potential distribution. Int J Heat Mass Transf 46:1541–1543

Lorente S, Wechsatol W, Bejan A (2002) Tree-shaped flow structures designed by minimizing path lengths. Int J Heat Mass Transf 45:3299–3312

Lorenzini G, Biserni C, Isoldi LA, Dos Santos ED, Rocha LAO (2011) Constructal design applied to the geometric optimization of Y-shaped cavities embedded in a conducting medium. J Electron Packag 133(4):041008–041008

Lorenzini G, Biserni C, Garcia FL, Rocha LAO (2012a) Geometric optimization of a convective T-shaped cavity on the basis of constructal theory. Int J Heat Mass Transf 55:6951–6958

Lorenzini G, Garcia FL, Santos ED, Biserni C, Rocha LAO (2012b) Constructal design applied to the optimization of complex geometries: T-Y shaped cavities with two additional lateral intrusions cooled by convection. Int J Heat Mass Transf 55:1505–1512

Lorenzini G, Biserni C, Link FB, Isoldi LA, Dos Santos ED, LAO R (2013) Constructal design of T-shaped cavity for several convective fluxes imposed at the cavity surfaces. J Eng Thermophys 22(4):309–321

Lorenzini G, Biserni C, Estrada ESD, Dos Santos ED, Isoldi LA, Rocha LAO (2014a) Genetic algorithm applied to geometric optimization of isothermal Y-shaped cavities. J Electron Packag 136:031011-1–031011-8

Lorenzini G, Biserni C, Link FB, Dos Santos ED, Isoldi LA, Rocha LAO (2014b) Constructal design of isothermal X-shaped cavities. Therm Sci 18(2):249–356

McGhee GR (2011) Convergent evolution: limited forms most beautiful. The MIT Press, Cambridge, MA

Neagu M, Bejan A (2001) Constructal placement of high-conductivity inserts in a slab: optimal design of "roughness". J Heat Transf 123:1184–1189

Pence DV (2002) Reduced pumping power and wall temperature in microchannel heat sinks with fractal-like branching channel networks. Microscale Thermophys Eng 6:319–330

Rocha LAO, Lorenzini G, Biserni C, Cho Y (2010) Constructal design of a cavity cooled by convection. Int J Design Nat Ecodynam 5:212–220

Tondeur D, Luo L (2004) Design and scaling laws of ramified fluid distributors by the constructal approach. Chem Eng Sci 59:1799–1813

Vargas JVC, Bejan A (2002) The optimal shape of the interface between two conductive bodies with minimal thermal resistance. J Heat Transf 124:1218

Wechsatol W, Lorente S, Bejan A (2001) Tree-shaped insulated designs for the uniform distribution of hot water over an area. Int J Heat Mass Transf 44:3111–3123

Wechsatol W, Lorente S, Bejan A (2002a) Optimal tree-shaped networks for fluid flow in a disc-shaped body. Int J Heat Mass Transf 45:4911–4924

Wechsatol W, Lorente S, Bejan A (2002b) Development of tree-shaped flows by adding new users to existing networks of hot water pipes. Int J Heat Mass Transf 45:723–733

Wechsatol W, Lorente S, Bejan A (2005a) Tree-shaped networks with loops. Int J Heat Mass Transf 48:573–583

Wechsatol W, Lorente S, Bejan A (2005b) Tree-shaped flow architectures: strategies for increasing optimization speed and accuracy. Numer Heat Transfer, Part A 48:731–744